Low-Speed Salient-Pole BLDC-Machine Control by Using a Single Sensor

Frederik De Belie[1], Jeroen De Backer, Araz Darba and Jan Melkebeek
Dept. Electrical Energy, Systems & Automation, Ghent University, Sint-Pietersnieuwstraat 41, 9000 Gent, Belgium
[1] corresponding author, tel: +32 9 264 79 14, fax: +32 9 264 35 82, e-mail : Frederik.DeBelie@UGent.be.

***Abstract*— This paper discusses an enhancement for salient-pole brushless dc-drives using a single current sensor in the dc-bus. The improvement is made by replacing the hall sensors with a rotor-position estimator, increasing the reliability of the drive and reducing its cost. As a result, the BLDC-drive is controlled by using a single sensor only, requiring a minimum amount of electronics to process the measurements. The additional advantage of a position estimator in BLDC-drives is the high resolution in the rotor position information. This allows to use advanced model-based controllers (e.g. programmed current control) and to extend the range of operation (e.g. higher speed by field weakening).**

I. Introduction

Recent advancements in electrical drives have reduced the number of sensors, either by reducing the amount of current sensors to a single one in the dc-link [2] or either by using self-sensing or sensorless methods [3]. Self-sensing or sensorless control refers to methods avoiding rotor-position sensor(s) by using a rotor-position estimator. This paper discusses an enhancement for salient-pole BLDC-drives by using a single current sensor in the dc-bus and by replacing the hall sensors with a rotor-position estimator. A contribution of this paper is the estimation of the rotor position from measurements obtained from a single current sensor, placed in the dc-bus. The additional advantage of a position estimator in BLDC-drives is the higher resolution in the rotor position information compared to the hall-sensor output. This allows to use advanced model-based controllers (e.g. current programmed control) and to extend the range of operation (e.g. higher speed by field weakening). The disadvantage of todays rotor-position estimators compared to position sensors is the decreased accuracy in the rotor position and hence commutation instances, resulting in a larger torque ripple. However, the back-emf in salient-pole BLDC-machines differs from the trapezoidal waveform. As a result, a small deviation in the commutation moments can be allowed as it has a small influence on the torque generation and power output. The requirement of an estimator is a more powerful controller as the technology demand shifts from hardware (sensors) to software (estimator).

II. Sensorless Current Control

An overview of the sensorless salient-pole BLDC-drive is given by the scheme shown in Fig. 1. A three-phase voltage-source inverter is used as switching converter to supply power to the salient-pole brushless dc-machine. The controller has two parts, a conventional current controller and the position estimator. The BLDC-drive is equipped with a single sensor in the dc-bus only, measuring the dc-current. The current controller is a digital predictive current controller or current

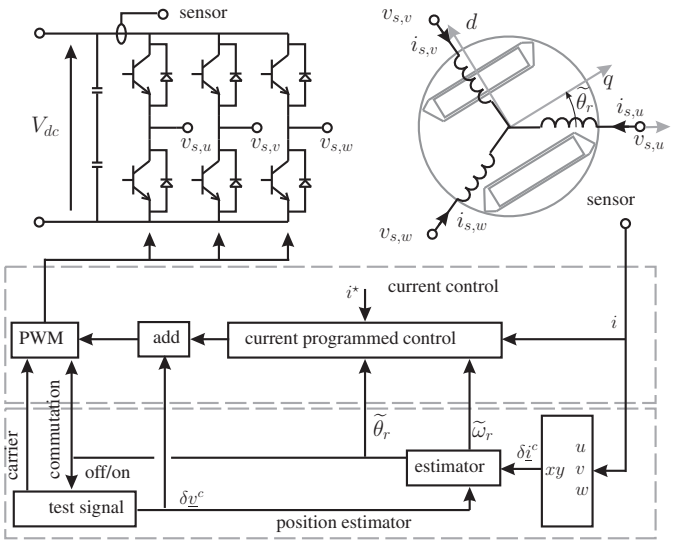

Fig. 1: Overall scheme of the sensorless current controller.

programmed controller and requires values for stator resistor, rotor position, inductance and back-emf. Besides current samples taken for current control, additional current samples are taken to measure the current ripple used in the rotor position estimator. A measurable current ripple is obtained by adding signals to the current controller output. The estimator can modify the PWM carrier in order to reconstruct the phase currents from samples taken by the single current sensor.

A different rotor-position estimator is used at low and high rotor speed. At higher speed (above 10% of nominal speed), it is advised to use the back-emf. An overview of back-emf based sensorless methods for BLDC-drives can be found in [5]. As these estimation methods are well-known, this paper will deal with the low-speed estimation only. The estimator at low speed obtains the rotor position from measurements of the current ripple caused by the phase voltages switching between the positive and negative side of the dc-bus voltage. For salient-pole machines this current ripple depends on the rotor position, the largest ripple amplitude for voltage vector variations along the axis of smallest inductance which is the d-axis or axis of the permanent magnets. In order to estimate the rotor position with sufficient accuracy the current ripple is increased by introducing deviations in the controller output. In [3], an enhancement is discussed for which the current samples of normal control aren't affected by the controller output deviations. This method is referred to as seamless integration

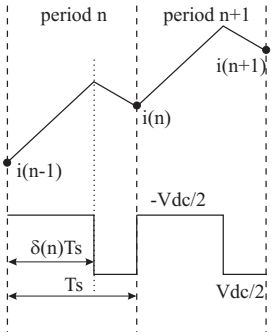

Fig. 2: Current programmed control: current and voltage

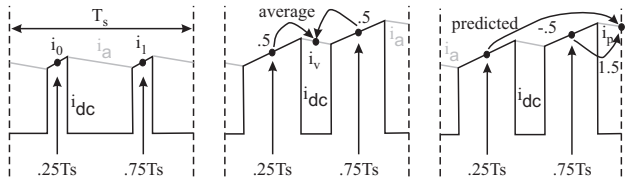

(a) during steady state (b) during transient, average current over PWM-period (c) during transient, predicted current at end PWM-period

Fig. 3: dc-current i_{dc} and phase current i_a, samples at 25% and 75% of PWM-period

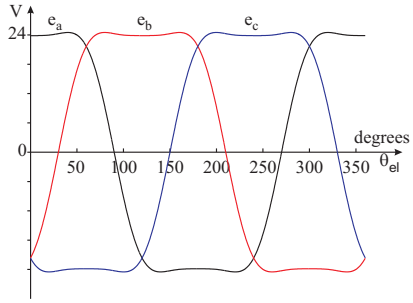

Fig. 4: Three-phase back-emf at nominal speed

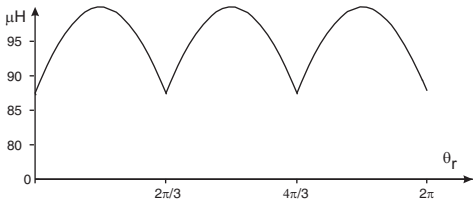

Fig. 5: Current programmed control: inductance as a function of rotor position

of the sensorless method in the current control loop.

Particular attention is given to the current commutation. During and after this period the current ripple can be distorted due to a strong variation in the controller output. As the estimator is used to detect the commutation moments, an estimation error affects on its turn the current commutation. The problem is illustrated in Fig. 12(a), the 60 degrees commutation threshold is crossed several times by the estimated rotor position, resulting in a distorted current commutation shown in Fig. 12(b). To solve this, during commutation, test signal injection will be removed. A commutation method will be discussed to reduce the current distortion due to commutation, resulting in a better position estimation also.

A. Current Programmed Controller

In six-step BLDC-drives the converter is steered in order to have a current flowing in two phases only. After each rotor displacement of sixty degrees a phase commutation of the current occurs. The amplitude of the current is controlled in order to generate the desired torque. In [4], a predictive digital current programmed controller for a single-phase switching converter is discussed. The current controller is applied here to BLDC-drives by taking into account the most important harmonics in the back-emf, Fig. 4 as well as the main magnetic saliency in the machine. As the latter two depend on the rotor speed and position, a sensor is often applied, replaced here by a position estimator and speed observer. As the current commutates between the phases, the phase inductance values has to be known over 120 degrees only, resulting in a periodic function of the rotor position as shown in Fig. 5. The back-emf is obtained from the estimated speed and open-circuit induced voltage at nominal speed, stored in a look-up table.

To control the amplitude of a current flowing through two phases only, often the lower transistor of one inverter leg is closed (duty ratio equals one), while the upper transistor of another inverter leg switches in order to chop the dc-bus voltage to the desired phase voltage. In this paper, in order to reconstruct the three-phase currents from the dc-bus current, this conventional switching scheme is replaced by a centered PWM scheme and by complementary switching of the lower and upper transistors as is done in AC-drives. The duty ratio δ of the phase with positive current equals the controller output ($0.5 \leq \delta \leq 1$), while the duty ratio of the phase with negative current is given by the complementary value $\delta^\star = 1 - \delta$. The resulting dc-current and phase current are shown in Fig. 3 for a single PWM-period T_s. Samples are taken of the dc-current at 25% and 75% of the PWM-period from which the average phase current in that PWM-period is computed:

$$i_v(n+1) = .5i_0(n) + .5i_1(n). \tag{1}$$

The average current can be used to compute the current ripple in the sensorless algorithm. For the purpose of predictive current control, the value of the current at the end of a PWM-period is predicted by

$$i_p(n+1) = 1.5i_0(n) - .5i_1(n) \tag{2}$$

The current at the end of the PWM-period can be written as the current at the end of previous PWM-period added with a variation Δi. This variation is caused by the volt-second variation with respect to the steady-state voltage $v_r = Ri_r + e_m$ where R is the total stator resistor and e_m is the induced voltage of the two phases through which the steady-state current i_r flows. As in the proposed PWM method, during the period $(2\delta - 1)T_s$ the voltage V_{dc} is applied and during the remaining PWM-period $(2-2\delta)T_s$ the voltage is zero over the two-phases, it follows that

$$i(n+1) = i(n) + \Delta i(n) \tag{3}$$

where the current varation of PWM-period n is given by

$$\Delta i = \frac{V_{dc} - v_0}{L}(2\delta(n) - 1)T_s - \frac{v_0}{L}(2 - 2\delta)T_s. \tag{4}$$

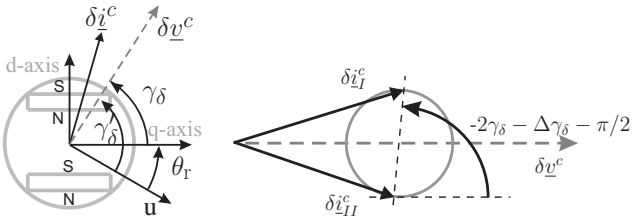

(a) Supplied voltage deviation $\delta\underline{v}^c$ and current response $\delta\underline{i}^c$ in the qd-reference frame fixed to the rotor.

(b) Set of current responses for test signals $\delta\underline{v}^c$ of equal modulus and different angle γ_δ.

Fig. 6: Average space vectors used in sensorless control

From this, the duty ratio $\delta(n)$ can be obtained which resulted in PWM-period n in the current variation $\Delta i(n) = i(n+1) - i(n)$

$$\delta(n) = \frac{L}{2T_s V_{dc}}\Delta i(n) + \frac{V_{dc} - v_0}{2V_{dc}}. \tag{5}$$

Using this equation for the duty ratio $\delta(n+1)$ of the next PWM-period, a system of two equations is obtained from which the current $i(n)$ van be eliminated. Then, controlling the current so that $i(n+1)$ equals the desired value $i^\star$, requires a duty ratio in PWM-period $n+1$ that equals

$$\delta(n+1) = \frac{L}{2T_s V_{dc}}(i_c - i(n-1)) + 1 - \delta(n) + \frac{v_0}{v_{dc}}. \tag{6}$$

B. Estimation of the PMSM rotor position

In a salient-pole PMSM the phase inductances vary strongly with the rotor position. As a result, the response of the phase currents on a voltage deviation from the controller output depends on the rotor position. Based on this voltage deviation, in [1], a low-speed position estimator is implemented on a voltage-source inverter (VSI) supplied PMSM. In practice, the voltage deviations are generated by modifying the width of the pulsed phase voltages. By measuring the current ripple caused by the average voltage deviation, an estimation of the rotor position is made for the purpose of vector control.

In the following, space vectors are used that correspond to the average value over a time period τ. For sufficiently small times, the linear small-signal machine model is valid by good approximation. Hence, the current difference over a time τ and caused by a pulsed test signal can be computed by the test signal average value over τ. The waveform of the test signal has no influence on the current difference and in this paper a pulse train is used generated by a switching converter. In case the test signals are generated by using a VSI with PWM, it is convenient to choose the PWM-period or half the PWM-period as period τ. In that case, the average component of the test signal is controlled by the duty ratio that steers the PWM.

In [1], average space voltage vectors, with components v^c_{q}, v^c_{d} in the synchronous qd-reference frame, are used in order to represent the test signals. The voltage deviations δv^c_{q}, δv^c_{d} from the steady-state voltage $v_{q,0}$, $v_{d,0}$ are denoted by δv^c_{q} and δv^c_{d} respectively. It is then shown that the resulting current variations δi^c_{q}, δi^c_{d} after a time $\tau << min(\tau_{\mathrm{q}}, \tau_{\mathrm{d}})$, with $\tau_{\mathrm{q}}, \tau_{\mathrm{d}}$ the synchronous time constants of q- and d-axis, can be approximated by

$$\delta i^c_{\mathrm{q}} = \frac{\tau}{L_{\mathrm{q}}}\delta v^c_{\mathrm{q}} \text{ and } \delta i^c_{\mathrm{d}} = \frac{\tau}{L_{\mathrm{d}}}\delta v^c_{\mathrm{d}}, \tag{7}$$

independent of the stator resistor R_{s} as well as rotor speed Ω.

To estimate the rotor position θ_r, an auxiliary angle is used: the angle γ_δ of the voltage vector $\delta\underline{v}^c(\delta v^c_{\mathrm{q}}, \delta v^c_{\mathrm{d}})$ with respect to the q-axis, Fig. 6(a). As the set value of the voltage test vector is computed by the current controller, its direction is known in the stationary $\alpha\beta$-reference frame and given by γ'_δ. From this and by estimating the auxiliary angle γ_δ, an estimation of the rotor angle θ_r is obtained as $\widetilde{\theta}_r = \gamma'_\delta - \widetilde{\gamma}_\delta$ where $\widetilde{x}$ denotes the estimation of x.

The set of current responses for test vectors of equal modulus and for $\gamma_\delta = 0 \ldots 2\pi$ is shown in Fig. 6. This set of responses is positioned on a circle and is often used in sensorless methods to estimate the rotor angle θ_r. A parameterless estimation method is used. For this purpose, the current response on a second test vector is measured. From the first test period, a current response $\delta\underline{i}^c_{xy,\mathrm{I}}(\delta i^c_{x,\mathrm{I}}, \delta i^c_{y,\mathrm{I}})$ is measured. The modulus of the second test vector deviation $\delta\underline{v}^c_{\mathrm{II}}$ is chosen equal to the modulus of the first test vector deviation $\delta\underline{v}^c_{\mathrm{I}}$: $\Delta v^c_{II} = \Delta v^c_I = \Delta v^c$. However, the vector deviation $\delta\underline{v}^c_{II}$ has a direction of $\gamma_\delta + \Delta\gamma_\delta$. The auxiliary angle γ_δ has been previously computed as a function of the current responses and is given as

$$\widehat{\gamma}_\delta = \frac{1}{2}\arctan\frac{\delta i^c_{y,\mathrm{I}} - \delta i^c_{y,\mathrm{II}}}{\delta i^c_{x,\mathrm{II}} - \delta i^c_{x,\mathrm{I}}} - \frac{2\Delta\gamma_\delta + \pi}{4}. \tag{8}$$

The sensorless method discussed here can be used in many ways. A possible implementation is given in Fig. 7 showing the duty ratios, resulting phase voltages and phase currents. The dashed lines correspond to half a PWM-period. Each three PWM-periods, test signals are avoided for a single PWM-period during which the average current is measured. From this average current value the predictive controller computes the steady-state duty ratio for the next three PWM-periods. During the two PWM periods that follows the PWM in which the average current is measured, test signals are added to the steady-state duty ratio. For the six-step BLDC-drive, one phase has an average zero value as can be seen in this figure. The current ripple due to the injection of test signals is clearly visible. An advantage of the sensorless method discussed here, is the negligible influence of the test signals on the average current. The current values before and after a test period in which test signals are injected are the same which benefits the controller as well as the estimator performances.

C. Using a single sensor

Test signals are applied in order to introduce a measurable ripple from which the position can be estimated. In Fig. 8(a), the phase current, dc-current and sampled dc-current at 25% and 75% of each PWM-period are shown. By using the aforementioned sensorless current controller, it follows that the dc-current amplitude corresponds to the amplitude of a single phase only, i.e. Δi_b in Fig. 8(a). To measure the three-phase current ripple from samples taken by a sensor in the dc-bus only, a modified PWM-scheme can be used. By modifying the

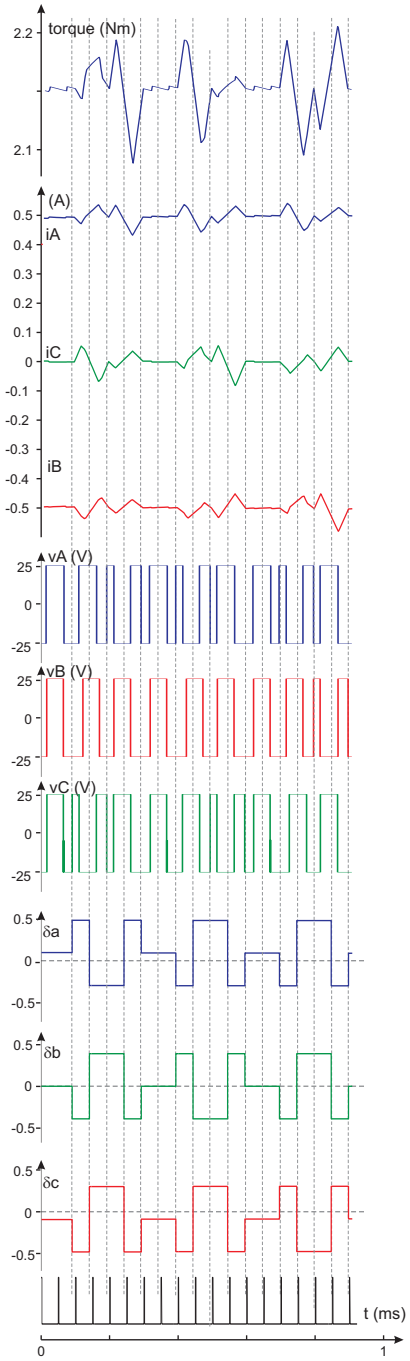

Fig. 7: Waveforms of duty ratios, voltages and currents.

PWM-modulation of one phase from centered to tailing edge or by inverting the PWM-carier for a single PWM-period, it follows that the dc-current can be used to measure two phases during a test period. This is shown in Fig. 8(b). Sampling the dc-current at the end of the PWM-period results in a sample of the a-phase and c-phase. As the sum of phase currents is equal to zero, the b-phase current can be computed. A disadvantage of this method is the delay between samples taken for each phase. However, signal-injection methods are mostly used at low speed for which the rotor position variation over several PWM-periods could be neglected and hence introduces small estimation errors.

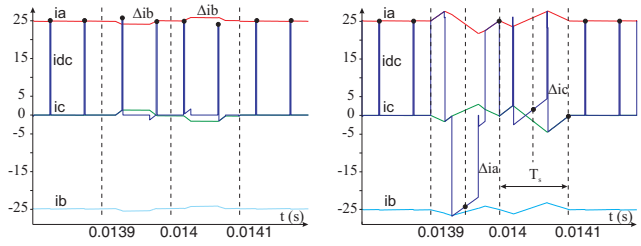

(a) fixed sampling moments at 25% and 75% of PWM-period

(b) modified sampling moments during test PWM periods

Fig. 8: Sampling of dc-current

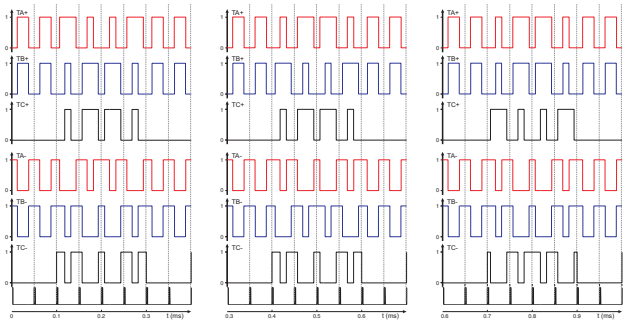

(a) devations along u-phase

(b) devations along v-phase

(c) devations along w-phase

Fig. 9: Stearing signals to generate voltage vector deviations, centered PWM

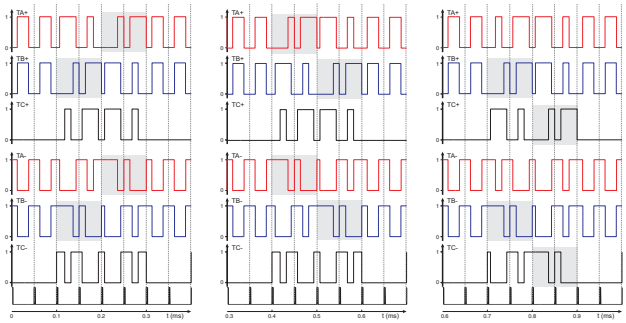

(a) devations along u-phase

(b) devations along v-phase

(c) devations along w-phase

Fig. 10: Stearing signals to generate voltage vector deviations, tailing edge PWM

Many PWM-modifications can be developed in order to measure the phase currents from a single current sensor in the dc-bus. One possible case is given in Figs. 9-10 showing the steering signals for the six transistors in the case of a centered PWM-method and a modified PWM-method. Gray areas show the differences between both strategies.

D. Commutation

Previous sections discussed the sensorless predictive current controller for which the current is controlled to a given value $i^{\star}$. This section deals with the period during which the current commutates from one phase to another. As mentioned before, test-signal injection is avoided during commutation. In most BLDC-drives, the commutation is done by using a duty ratio equal to one as the maximum voltage results in a fast commutation. However, such strategy affects the

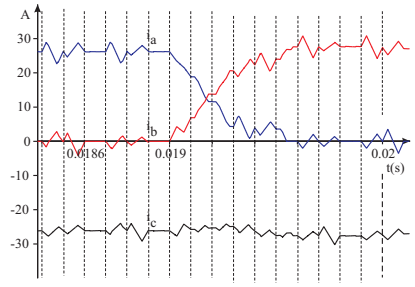

(a) Three-phase current during commutation

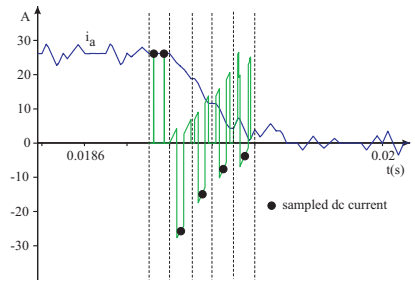

(b) dc-current samples in order to control the current during commutation

Fig. 11: Commutation of the current

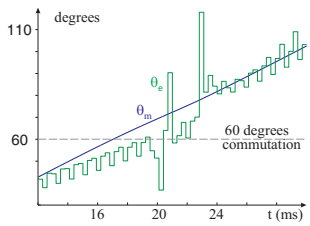

(a) Rotor-position estimation

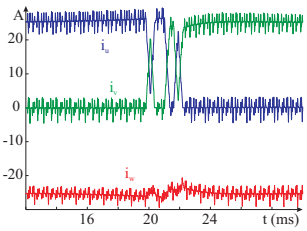

(b) Phase currents

Fig. 12: Current commutation in a sensorless BLDC-drive, mutiple undesired commutations

currents, resulting in current overshoot and an important torque transient. A better response is obtained here by computing the duty ratio during commutation in such way the time gradient of the current rise in one phase equals the negative time gradient of the current drop in the other phase. As a result of this strategy, the third phase current is less affected by the current commutation compared to more classic methods. This is shown in Fig. 11(a), clearly during commutation of the current from the a-phase to the b-phase, the current in the c-phase is with little influence. To obtain the average-current values during commutation, it can be required to take samples of the dc-current at 50% of each PWM-period as shown in Fig. 11(b). Samples at 25% and 75% of the PWM-period should be taken when the current varies from negative values to zero.

Sensorless control can be affected by the commutation instances resulting in strong variations in the estimated rotor position and hence multiple undesired commutation instances and distorted phase currents as shown in Fig. 12. The estimated rotor position is affected by noise also due to neglecting the influence of sample delays, switching dead time and stator resistor on the current ripple. Fig. 13 shows the estimated rotor position θ_e.

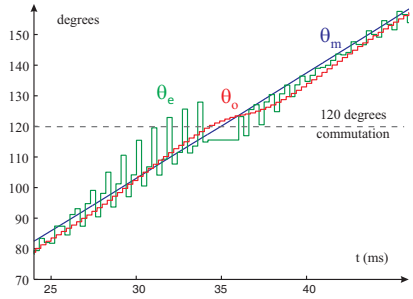

Fig. 13: Estimated θ_e and filtered θ_o rotor position

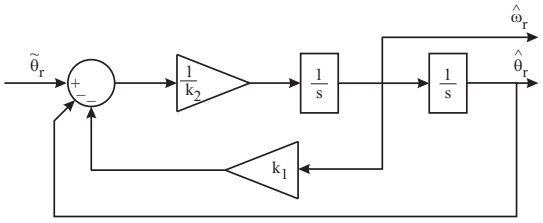

Fig. 14: Second-order observer to observe the speed and filter the position.

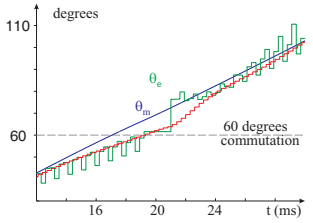

(a) Rotor-position estimation

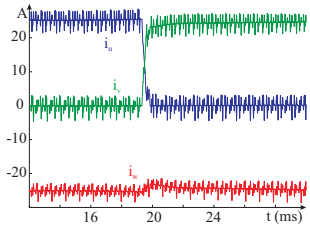

(b) Phase currents

Fig. 15: Current commutation in a sensorless BLDC-drive, single commutation

To solve this problem, a second-order observer is used, Fig. 14, observing the rotor speed and filtering the rotor position as shown by θ_o in Fig. 13. Moreover, during commutation, the sensorless method is placed on hold and the rotor position is estimated by extrapolation of previous estimations. For this purpose, the observed speed can be used. Applying this strategy results in the current commutation as shown in Fig. 15, clearly the phase currents are less distorted.

III. Simulations

The algorithms aforementioned are programmed by using Simulink® within the Matlab® environment of MathWorks®. The BLDC-machine and converter are modelled by using PLECS® of Plexim GmbH. A BLDC model is used taking into account the main important harmonic content of both back-emf and phase inductance. The converter is supplied with a dc-voltage of 36V, switching frequency equals the PWM frequency of 10 kHz. The phase inductance varies between 50 μH and 100 μH, the stator resistance R=15$m\Omega$, the back-emf at nominal speed is given in Fig. 4, the machine has a small inertia of 180 μkgm^2. Test signals are injected for which the duty ratio deviation from steady state is 0,2.

Simulation results are shown in Figs. 16-19. One phase current for an electrical period is shown in Fig. 16. The current ripple as result of test signals is clearly visible. The

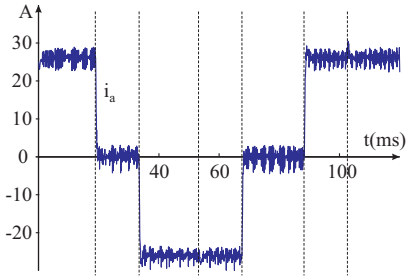

Fig. 16: Phase current a

commutation is swift, approximates the performance of a dead-beat control and is without overshoot in the current. The commutation of the current occurring between 40ms-60ms has little influence on the phase-current. This is an advantage of the commutation method discussed before. The estimated as well as filtered rotor position are shown in Fig. 17 and the filtered values are used to determine the instances of current commutation. The differences with the real rotor position are shown in Fig. 18. The error is periodic over 120 electrical degrees and is maximum 10 electrical degrees.

The commutation moments are given by vertical lines in Fig. 16 and the time difference between commutation instances varies. The errors in the commutation moments affect the speed and torque as shown in Figs. 19-20 respectively. A variation in the torque could be expected due to the saliency of the BLDC-machine. Additional to these variations, drops can be noted in the torque during the commutation instances. This is a result of the errors in the estimated rotor position and a well-known issue to be solved. As the machine has a small inertia of 180 μkgm^2, torque ripples influence the rotor speed noticeable. From Fig. 20 it follows that even the current ripple affects the rotor speed. Despite these variations, the drive is stable and the average speed and torque can be steered by the sensorless current control loop.

IV. Conclusions

Low-speed current control for salient-pole BLDC-machines by using a single current sensor has been discussed. Test signals are seamlessly injected in order to introduce a measurable ripple from which the rotor position can be estimated. A predictive current controller is discussed based on a rotor-position based machine model. Particular attention is given to the current control and rotor position estimation during commutation instances. These methods have been developed based on samples of a single sensor only, placed in the dc-bus, resulting in less electronic components. Senorless control of BLDC-machines is still affected by errors in the commutation instances resulting in torque drops. Nevertheless, it is shown by simulations that sensorless current control by using a single sensor can operate a salient-pole BLDC-machine in a stable way.

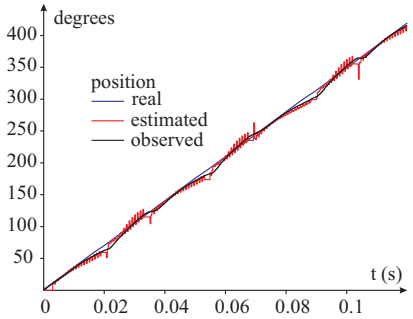

Fig. 17: Rotor position for one electrical period

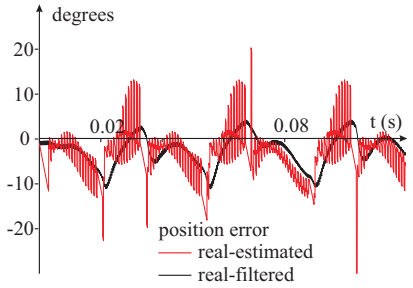

Fig. 18: Rotor position error for one electrical period

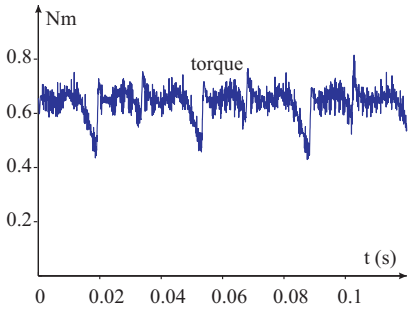

Fig. 19: Torque for one electrical period

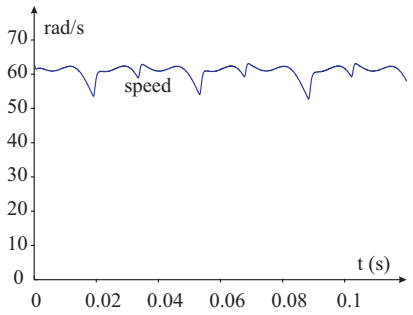

Fig. 20: Rotor speed for one electrical period

References

[1] F. De Belie, P. Sergeant and J. Melkebeek, A Sensorless Drive by Applying Test Pulses Without Affecting the Average-Current Samples, IEEE Transactions on Power Electronics, Vol. 24 (4), April 2010, pp. 875–888.

[2] J.I. Ha, "Current Prediction in Vector-Controlled PWM Inverters Using Single DC-Link Current Sensor," IEEE Transactions on Industrial Electronics, Feb. 2010, Vol. 57(2), pp. 716–726.

[3] F. De Belie, P. Sergeant and J. Melkebeek, "A Sensorless Drive by Applying Test Pulses Without Affecting the Average-Current Samples," "IEEE Transactions on Power Electronics, April 2010, Vol. 25(4), pp. 875–888.

[4] J. Chen, A. Prodic, R. Erickson and D. Maksimovic, "Predictive Digital Current Programmed Control," IEEE Transactions on Power Electronics, Jan. 2003, Vol. 18(1), pp. 411–419.

[5] P. Acarnley and J. Watson, "Review of Position-Sensorless Operation of Brushless Permanent-Magnet Machines," IEEE Transactions on Industrial Electronics, April 2006, Vol. 53(2), pp. 352–362.